Dynamics of molecular reactions in solids: Photodissociation of HI in crystalline Xe

R. Alimi, R. B. Gerber, and V. A. Apkarian

Citation: The Journal of Chemical Physics **89**, 174 (1988); doi: 10.1063/1.455501
View online: http://dx.doi.org/10.1063/1.455501
View Table of Contents: http://scitation.aip.org/content/aip/journal/jcp/89/1?ver=pdfcov
Published by the AIP Publishing

Dynamics of molecular reactions in solids: Photodissociation of HI in crystalline Xe

R. Alimi and R. B. Gerber
Department of Physical Chemistry, The Fritz Haber Research Center for Molecular Dynamics, The Hebrew University of Jerusalem, Jerusalem 91904, Israel

V. A. Apkarian[a)]
Department of Chemistry, Institute for Surface and Interface Science, University of California, Irvine, California 92717

(Received August 18 1987; accepted 15 March 1988)

The photodissociation of HI impurities in a crystalline Xe host is studied by molecular dynamics simulations. From the calculated trajectories, analyses are given for: The behavior of the HI molecule before dissociation, the motions of the fragments following photon absorption, and the sites and vibration dynamics of the H fragments long after dissociation. The main findings include: (i) The photodissociation yield as a function of temperature is not monotonic (0 at 0 K, 0.2 at 17 K, 0.1 at 35 K). (ii) The nascent H atoms, at early time ($\sim$0.5 ps), exhibit well defined, high frequency ($\sim$900 cm^{-1}) vibrations in the cage. The H trajectories acquire increasingly a random walk character with the progress of time. (iii) H exit from the cage is virtually never direct. (iv) After relaxation to equilibrium, the product H atoms occupy dilated interstitial sites (nearest-neighbor xenons displace by 0.3 and 0.6 Å at the octahedral and tetrahedral interstitial sites, respectively). (v) The H atom dynamically distorts the octahedral site and exhibits three well-separated local vibrational frequencies, corresponding to motions along well-defined axes of the site. (vi) The reagent HI molecular rotations are strongly hindered at low temperatures, and are more aptly described as large amplitude bendings associated with the complex Xe$\cdots$HI. The experimental implications of the above findings and the possible consequences of quantum effects are discussed.

I. INTRODUCTION

The topic of molecular reaction dynamics in crystalline solids raises some fascinating prospects and questions. A prime motivation for pursuing this subject is that it may offer important insights into the broader field of reaction dynamics in condensed matter. Efforts at theoretical understanding of such processes at the microscopic level have been pursued extensively for liquid solutions.[1] It can be argued that a first-principles understanding should be more easily reached for reactions in a crystalline host, since the structural properties of crystals are much simpler than those of liquids. Reactions in solids are also interesting for several other reasons. For example, pronounced effects in reactivity due to frozen geometries is to be expected and should be possible to study with rigor. The fact that molecular rotations, and often other large amplitude motions, are arrested in low-temperature solids, suggest that effective density of states for processes in such systems can be quite low compared with that pertinent to liquids. This indicates a likelihood of nonstatistical state-selective behavior for reactions in low temperature solids. Another interesting prospect is that important tunneling effects may be found for some reactions at very low temperatures.

So far, experiments of chemical reaction dynamics of small molecular species in a single crystal or in polycrystalline media have not been reported (studies in crystalline environment have been carried out for electron transfer processes,[2] but these are very different from reactions involving chemical bond breaking). On the other hand, there has been much activity in experimental studies of molecular reactions in rare gas matrices,[3] materials which are not structurally well characterized, but may be similar in several properties to the corresponding rare-gas crystalline solids. For example, starting from the work of Baldeschwieler and Pimentel,[4] unimolecular rotational isomerization dynamics of guest molecules in rare-gas matrices was extensively pursued by several authors.[5–8] In particular, evidence for state selectivity was found by Shirk and Shirk in the isomerization of HONO,[7] and by Rasanen and Bondybey[8] for the rotomerization of Butane in Ne. Bimolecular reactions of guest molecules in rare-gas solids were studied, e.g., by Turner and Poliakoff[9] and by Frie *et al.*[10,11] Photodissociation of diatomic and small polyatomic molecules such as ICl and CH_3I were pursued by Bondybey and Brus[12,13] and Bondybey and Fletcher,[14] who focused on the very important question of the cage effect in reactions in solids. Photoinduced harpoon reactions of halogens in matrices were recently explored by Apkarian and Fajardo.[15–17] They demonstrated efficient and permanent photodissociation of molecular halogens and hydrogen halides via the ionic charge transfer potentials. Given that matrices are not as structurally well defined as are crystalline solids, an important challenge for future research is to pursue photochemical reactions in single-crystal hosts. To this end, the experimental studies at Irvine have been extended to high pressure cryocells in which transparent solids of high optical quality (albeit poly-

a) Author to whom you should address correspondence to.

 0021-9606/88/130174-10$02.10

crystalline) are prepared by slow freezing of rare-gas solutions.[17]

In the absence of experiments on reaction dynamics in single crystals, there seem to have been no theoretical studies on such systems either. Several models were developed for the topic of vibrational energy relaxation of impurity molecules in solids, a subject related to reaction dynamics in such systems.[18–21] Although the experimental findings that motivated the theories were all obtained in matrix studies,[22] the models proposed invariably assumed an isolated impurity in an otherwise crystalline environment. Recently, Alimi *et al.*[23] studied by molecular dynamics simulations the photodissociation of Cl_2 and HI in large rare-gas clusters (up to $\sim 10^3$ atoms), exploring the question of limiting behavior as cluster size is increased. That study was, however, limited to initial cluster temperatures of 0 K.

The purpose of the present study is to explore by molecular dynamics simulations the photodissociation of HI in a crystalline Xe host at finite temperature. The purpose of the simulations is to investigate the motions of the fragments throughout the process, to determine the physical mechanism whereby exit from the cage occurs, and to explore the structure and vibrational dynamics of the final sites in which the fragments are ultimately trapped. This study suggests observable features that may guide future experiments, and such experiments on photodissociation of HI in crystalline Xe are underway at present at the University of California at Irvine.

The structure of the article is as follows. The interaction potentials used and some details of the calculations are discussed in Sec. II. The results and their interpretation are presented in Sec. III. Implications of the work for future experimental studies, and the possible role of quantum effects are discussed in Sec. IV.

II. SYSTEM AND METHOD

The UV absorption spectrum of HI in the gas phase has been well studied.[24,25] The main dissociative absorption is due to a transition from the ground Σ_g^+ state to the excited $^1\Pi_u$ state, the latter having a purely repulsive character.[26] We shall assume that only $I(^2P_{3/2})$ atoms are produced in this process. Since our interest here is in photofragment motion following photon absorption, we shall adopt a simplistic quasiclassical description for the excitation, namely: a vertical transition of the HI molecule at its ground-state equilibrium configuration. This is modeled by a sudden switch of the interaction potential between H and I from the Σ_g^+ Morse to $^1\Pi_u$ exponentially repulsive potential. The motions of all particles are assumed to follow classical dynamics both before and after the transition. The assumption of classical mechanics for a low-temperature solid is suspect, especially for the light H fragment. Indeed, much of our interest in this system stems from the likelihood of finding substantial quantum effects. Nevertheless, classical dynamics is at least a very useful and interesting reference point. Quantal treatment of this same system, in which the hydrogen atom is modeled by wave propagation techniques, is now in progress.

We assume pairwise interactions between all the atoms involved. For the Xe/Xe interaction a Lennard-Jones potential calibrated from gas-phase data is used.[27] We assume that the $Xe/I(^2P_{3/2})$ interaction is the same as the Xe/Xe one, an assumption that seems reasonable for the repulsive part of the potential, although it is more doubtful for the attractive. The results are not expected, however, to be sensitive to this interaction. The assumed H/Xe potential:

$$V_{H/Xe}(r) = \frac{\epsilon}{\alpha - 6}\{6\exp[\alpha(1 - r/r_m)] - \alpha(r_m/r)^6\}, \tag{1}$$

where $\epsilon = 6.81$ meV, $r_m = 3.95$ Å, $\alpha = 14.28$, is from a fit to scattering data.[28] The repulsive $H(^2S_{1/2})/I(^2P_{3/2})$ interaction is taken as

$$V^*_{H/I}(R) = Be^{-\beta R}, \tag{2}$$

where the constants $B = 34.24$ eV, $\beta = 1.934$ Å^{-1} were obtained by fitting the $^1\Pi_u$ curve of Ref. 26. An important limitation of the treatment in this study is that it is strictly adiabatic. No allowance is made for curve hopping and subsequent recombination on the ground state potential: Nonadiabatic transitions from $^1\Pi_u$ to Σ_g^+ that may take place in principle throughout the process are ignored. A semiclassical treatment of this curve hopping process is in principle possible. However, requisite to such a treatment are the matrix elements coupling the two surfaces. Reliable mixing coefficients are not available for the isolated molecule, let alone a molecule trapped in the dense medium in which perturbations by the environment are to be expected to play a major role in coupling of surfaces. Fully realizing this shortcoming, solace is taken in the fact that in all cases in which the H fragment exits the cage, it does so with sufficient average kinetic energy ($\gtrsim 0.15$ eV), which guarantees the system to be sufficiently above the asymptotic crossing of potentials.

In the studies of HI photodissociation in Xe clusters[23] it was assumed that all the orientations of the HI within the cluster were equally probable. Here this assumption was not imposed, and as it turns out it is far from justified at low temperatures. In the present simulations, the orientation of the HI within the unit cell can affect the outcome of the photodissociation. Therefore, the motions and configurations of the HI molecule within the host crystal before photodissociation are studied for determining the appropriate initial conditions for the fragmentation process. In the absence of a reliable Xe/HI potential function, we opted for a choice offering simplicity; adopting a pairwise interaction (dumbbell potential):

$$V_{Xe/HI}(\mathbf{r}_{Xe},\mathbf{r}_H,\mathbf{r}_I) = V_{Xe/I}(\mathbf{r}_{Xe} - \mathbf{r}_I) + V_{Xe/H}(\mathbf{r}_{Xe} - \mathbf{r}_H), \tag{3}$$

where $\mathbf{r}_{Xe}$, $\mathbf{r}_H$, $\mathbf{r}_I$ are the position vectors of the three atoms involved. For the interatomic potentials $V_{Xe/I}$, $V_{Xe/H}$ we used the same functions as in the case where the molecule is dissociated. The H/I interaction in the prephotodissociation stage corresponds to the Σ_g^+ ground state, for which we used a Morse function calibrated by spectroscopic data.[29] The interaction potential (3) is unlikely to prove of quantitative accuracy, but its role in determining the photodissociation

dynamics is indirect, and the results in this respect should not be sensitive to the choice of that interaction.

Molecular dynamics simulations have become a technique of common use in the study of condensed matter properties and excellent accounts are available on their application to solid systems.[30] We therefore discuss here briefly only the specific adaptations considered here.

In the calculations reported here, the Xe atoms and the center of mass of the HI (before dissociation) were placed initially at substitutional fcc lattice sites. One hundred seven Xe atoms and the HI molecule were explicitly included in the calculations. The arrangement is such that there are six planes of Xe atoms cutting each of the directions (001); (010); (100), and the HI is at the center of the structure. The geometry around the HI substitutional site position is shown in Fig. 1. Periodic boundary conditions are imposed on the finite cluster described above, so as to approximate the effect of the bulk crystal on the subsystem explicitly incorporated in the calculations. The imposition of periodic boundary conditions on a finite cluster system can lead to difficulties for some systems. For instance, the onset of photodissociation in $Cl_2[Ne]_n$ clusters was found to lead to a cascade of interatomic collisions that propagate to the boundary of the cluster, as a shock wave.[23] The introduction of periodic boundary conditions at the cluster boundaries will cause a backreflection of the shock wave into the cluster resulting in unphysical artifacts—in extended crystalline matter, the shock wave will propagate further away from the reaction zone, and in time will undergo dispersion and damping. While this effect can be extremely important in some systems, it does not occur in HI photodissociation in Xe, probably due to the low hydrogen-to-xenon mass ratio:

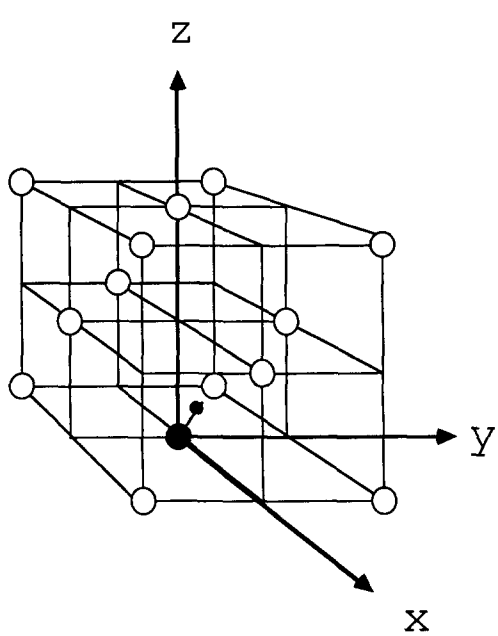

FIG. 1. Geometry of impurity molecule in an undistorted fcc host lattice (open circles = Xe atoms, shaded circle = I, filled circle = H). The angle θ in the text is the polar angle between the Z axis and the molecular axis. ϕ is the azimutal angle measuring the orientation of the projected molecular axis in the (x,y) plane.

the impact of the H photofragment on the neighboring atoms does not yield a sufficient amount of energy transfer for the onset of a shock wave.[23]

The initial orientation of HI in the simulation is taken such that the H atom is on a line joining the I and a xenon nearest neighbor. Velocities, randomly chosen from a Boltzmann distribution, are imparted initially to all atoms. The system is then allowed to evolve in time to equilibrate at a well-defined temperature. The temperature of the system is determined from the time averaged kinetic energy after equilibrium. The HI molecule is allowed to rotate, and when its thermal energy suffices to overcome the barrier for such motion, it will do so. This system of HI molecule in crystalline Xe is allowed to evolve in time for durations of the order of 25 ps, during which time it undergoes relaxation from the initial "exact" fcc structure. Configurations are chosen randomly from such a time file as initial conditions for the photodissociation. Photodissociation is assumed to take place instantaneously: The H–I interaction is suddenly switched to the repulsive $^1\Pi_u$ curve. The positions of the atoms are assumed not to change at the instant of photoabsorption, in the spirit of the Franck–Condon principle, neither is there a change in the momenta except that of the H–I mode. With these as initial conditions following photon absorption, the interpretation of the equations of motion in time is resumed, and pursued for a time scale of the order of 10 ps. At this point the H fragment has essentially relaxed in terms of its energy content, and a conclusion can be made whether it has left the original cage (reaction in our terminology) or whether it has remained, or returned there (nonreaction or recombination in our terminology). Twenty trajectories of photofragmentation were run at each temperature. Although the number is small, our tests indicate at least semiquantitative convergence with regard to the cage-exist probabilities, and certainly with regard to the qualitative physical features found. This is aided by the fact that at the studied temperatures, HI assumes a limited range of orientations with respect to the cage due to the strong hinderence of its rotational degrees of freedom. The integrations of the equations of motions were done using Cartesian coordinates, with standard integrator (D-Gear) methods.[31] In addition to analysis of the trajectories themselves, an important tool of interpretation was the Fourier transform of the trajectories, showing the relevant frequencies of the motions. These were obtained by using a fast Fourier transform algorithm. The calculations were done on a cluster of VAX 785/865 computers. The CPU time per trajectory was approximately 2 h.

III. RESULTS AND ANALYSIS

A. HI hindered rotation in crystal

An interesting aspect of the molecular behavior in the solid prior to dissociation pertains to its rotational motion. The question is whether, at a given temperature, that motion is free or hindered. The degrees of freedom pertinent to rotation are θ and ϕ, defined in Fig. 1. Consider now Fig. 2(a), which shows the time variation of θ for a typical trajectory at 17 K. After a brief transient following the initial configura-

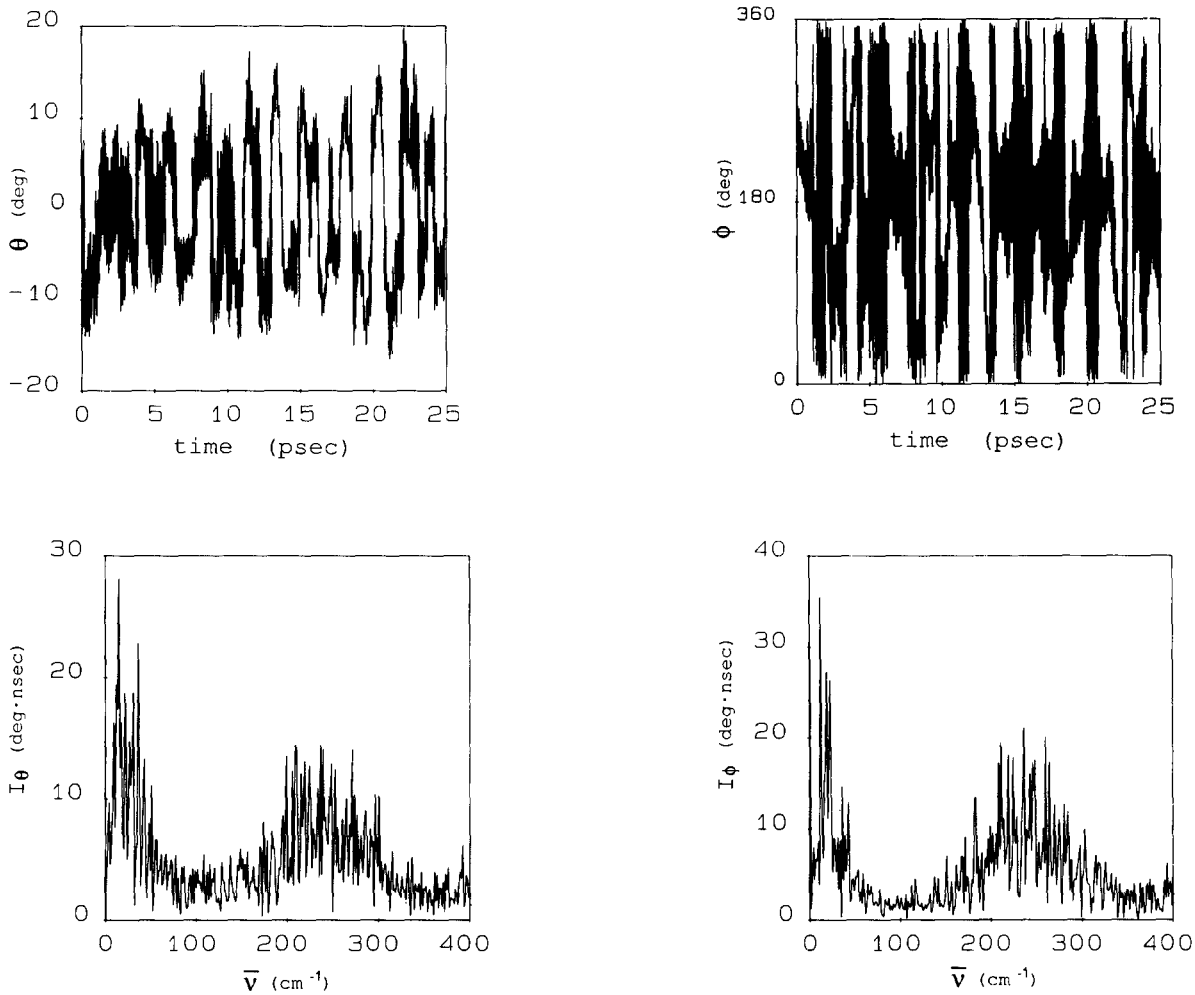

FIG. 2. Variation of the orientation angle θ. (a) Time variation of θ; (b) Fourier transform $I_\theta(\bar{\nu})$ of $\theta(t)$. The results are for HI in a 17 K Xe lattice.

FIG. 3. Variation of ϕ (at $T = 17$ K). (a) Time variation of ϕ; (b) Fourier transform $I_\phi(\bar{\nu})$ of $\phi(t)$.

tion, the basic θ motion exhibited is that of large amplitude ($\Delta\theta \sim \pm 20°$) vibration. Superimposed on the main vibrational structure are higher frequency motions. Figure 2(b) shows the Fourier transform of $\theta(t)$, $I_\theta(\bar{\nu})$. The frequency associated with the main oscillatory structure is in the range of 20–30 cm^{-1}. The fast, jittery oscillation superposed on the main vibrations peak in the frequency range of ~ 250 cm^{-1}. Figure 3(a) shows the time variation of the ϕ motion: here the basic picture is of full and nearly free rotation in that variable, but with fast jittery oscillations superposed on the main, slower time variation. As the Fourier transform $I_\phi(\bar{\nu})$ shows, the frequency structure is very similar to that of the θ motion. The interpretation suggested by Figs. 2 and 3 is that, qualitatively, the motion can to a large extent be understood in terms of a complex IH···Xe between the HI molecule and a neighboring Xe atom, the average configuration being the collinear one. θ corresponds obviously to the large amplitude bending of such a "complex," while ϕ describes the precession of the HI, in noncollinear configurations of the complex, around the I···Xe axis. θ and ϕ are, however, not good separable variables in this system, but are strongly coupled, so the same frequencies appear in both. The fast oscillations stem from the very anharmonic, large displacement regions of the effective potential in θ and ϕ. In following adiabatically the motions of the heavy atoms, the H enters into such regions of the potential, where the local frequency is very high, and where the H carries out the fast, transient jitters, before resuming the overall regular θ and ϕ oscillations.

The fact that the HI rotation in Xe is hindered and nonfree at 17 K appears somewhat surprising, since infrared spectra of hydrides in matrices is generally interpreted in terms of nearly free rotor states[22] (although the rotor levels can be shifted by coupling to localized phonons. See the rotational translational coupling model of Friedmann and Kimel.[31]) The free-rotor picture was developed, however, on the basis of rovibrational spectroscopy of HX molecules in matrices. The structure in a crystalline host solid, as modeled here, may be tighter, probing more anisotropic parts of the interaction potential between the molecule and neighboring atoms. It should be noted that a dumbbell model was employed in the present study for the HI/Xe potential, and that such potentials tend to be too anisotropic. Perhaps the real situation is thus nearer to the free-rotor picture. Also,

while we did not pursue this point in detail, at higher temperature ($T = 40$ K) much larger amplitudes were found for the θ motion, probably approaching full rotational behavior. This is in the spirit of the molecular dynamics simulations of Nosé and Klein[32] who found results corresponding to unrestricted motion in θ for a model consisting of 4 HCl molecules and 242 Ar atoms arranged on an fcc lattice. The temperature range explored in that study was above 30 K.

In conclusion, our studies of HI/Xe suggest not an isotropic distribution of the molecular orientation within the unit cell at 17 K, but rather something resembling a collinear complex IH···Xe of large amplitude bendings. There is definitely no free rotation or rotational diffusion at 17 K with the interaction potential used. We are currently pursuing the onset (as T is increased) of the transition to full rotational motion and to rotational diffusion. The result has important implications for the expected spectra of HI impurities in crystalline Xe, and related systems.

B. Effect of delayed exit from the cage

We proceed now to consider the photodissociation process itself. Figure 4 shows the path of a trajectory at 17 K that results in "reaction," i.e., in the nomenclature employed here, the exit of the H fragment from the original cage of surrounding Xe (and I) atoms, and the final relaxation (at least on the time duration of 20 ps) of that species in the new site within another cage. The path is shown as a projection on the Z and X' plane, where Z is the coordinate along the (0,0,1) direction, and X' is the coordinate along the (0,1,0) + 1/2(1,0,0) direction. An obvious important observation is that the exit from the cage is not direct upon photodissociation, *but follows considerable rattling in the original cage* (the duration of which is several ps), the confines of which in Fig. 4 are roughly $Z \lesssim 4.5$ Å, $X' \lesssim 1.5$ Å. Figure 5 shows the variation in time of the H atom distance from its initial position, for the same reactive trajectory as in Fig. 4. Three distinct regimes are clearly visible: One, of duration of the order of 3 ps, that involves oscillatory motions within the original cage (i.e., without getting far from the original configuration of the H atom when it was bound to the I). The large fluctuations in $|\mathbf{r}(t) - \mathbf{r}_0|$, reflect on the large amplitude rattling of the H within the original cage, that is evident also from the path in Fig. 4. Then, there is a sudden exit from the cage around $t = 3.5$ ps. Also this stage shows large oscillations in $|\mathbf{r}(t) - \mathbf{r}_0|$. Finally, for $t > 3.5$ ps the H moves in the new cage. The fluctuations in $|\mathbf{r}(t) - \mathbf{r}_0|$ have become much smaller since the H atom lost most of its energy at this stage and is confined to a much smaller range of configurations in the new, tighter T_d cage. Another perspective on the same process is given by Fig. 6, which shows the variation in time of the kinetic energy of the H photofragment for the same trajectory. Clearly there is a very rapid loss of most of the kinetic energy gained after photodissociation on a time scale of 0.1 ps. The kinetic energy left at this stage is considerably above equilibrium value. Over the time range between 1 ps (after the photon absorption) and 3.5 ps the mean kinetic energy drops gradually, as a result of energy transfer to the Xe lattice. For $t > 3.5$ ps, the H atom is already in the new cage with relatively low residual kinetic

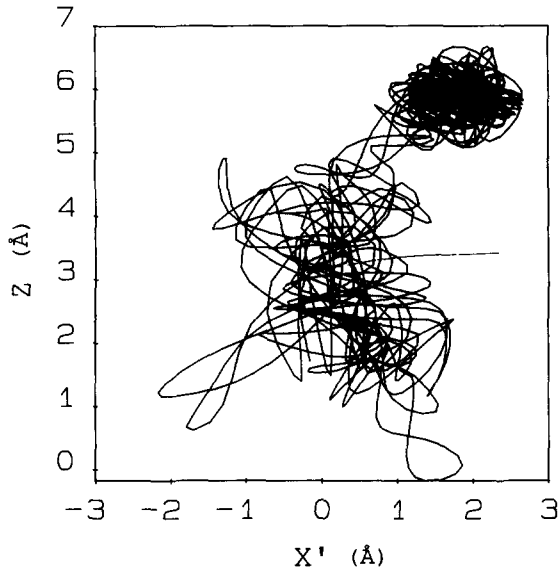

FIG. 4. Path of a reactive (cage exiting) trajectory of an H atom from photodissociation of HI in a 17 K Xe crystal. The result is for initial relative energy 1.5 eV of the photofragments. Z denotes the coordinate along the (0,0,1) axis of the fcc structure. X' is measured along the (0,1,0) + cos(60°) (1,0,0) axis.

energy, virtually relaxed to equilibrium. However, note that at the onset of cage exit, ~3 ps, the H atom contains an average of ~0.15 eV which makes the neglect of recombination a reasonably safe assumption. This picture is characteristic of all the reactive trajectories in this system: *Reaction due to photodissociation, in the sense of exit from the original cage, appears never to be a direct process.* Before the H atom finds a low barrier it can cross to reach the new cage, it covers by large amplitude vibrations much of the configuration space in the original cage, loosing most of the photodissociation energy by collisions to the "walls" of the cage. *The non-*

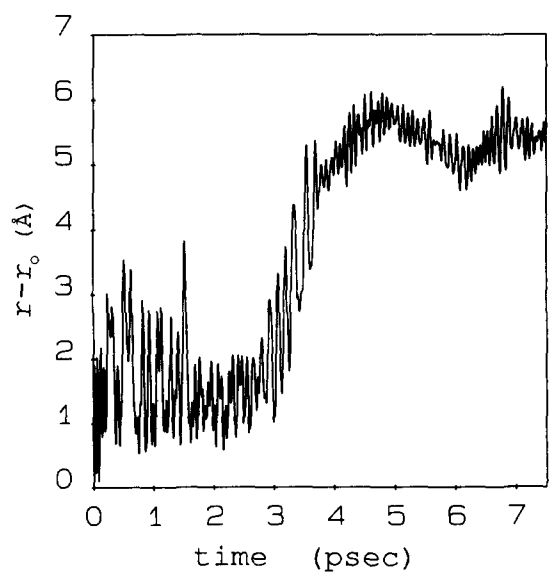

FIG. 5. Trajectory in time of H photofragment. The result is for photodissociation in a 17 K Xe lattice, initial energy of the photofragments being 1.5 eV. $|\mathbf{r}(t) - \mathbf{r}_0|$ measures the distance of H at time t from its initial position at the instant of photon absorption.

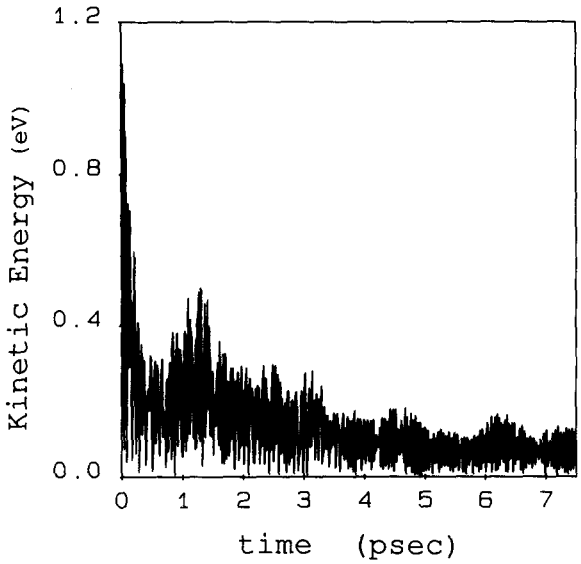

FIG. 6. Time dependence of the kinetic energy of the H photofragment. The result is for the same trajectory as in Figs. 4 and 5.

direct nature of the reaction, and the nature of the long "rattling" stage preceding it should have important consequences for the formulation of statistical theories dealing with cage exit and recombination in such systems.

C. Temperature dependence of cage-exit probability

Table I lists the calculated reaction (i.e., cage exit) probabilities for $T=0$ K, $T=17$ K, and $T=35$ K. The reaction probability, which is 0 at 0 K rises to 0.2 at $T=17$ K, then falls off to 0.1 for $T=35$ K. The interpretation of this behavior is as follows. Starting from $T=0$ K, increasing T lowers the barrier for H exit from the cage, since as the distance between two neighboring Xe atoms increases in the course of vibrational motion, the repulsion for H passage between them decreases. The effect of increasing temperature is thus to lower the effective barrier for cage exit by increasing the amplitudes of Xe vibrations. As the temperature is further increased, energy transfer from the Xe vibrations to the moving H atom becomes of increasing importance. Such energy transfer can induce the reverse reaction, i.e., return from the local minimum site in the new cage to the original one. The energy transfer can also affect the H atom before reaching the new cage by diverting the photofragment from its motion along the reaction path. The small number of reactive trajectories in our calculations makes it hard to draw any quantitative conclusions as to the most probable point along the reaction path at which the return of the H to the original cage is likely to occur. Nevertheless, the competing mechanisms that produce a maximum in the reaction probability in this case are quite general. We note that we did not pursue calculations for $T>35$ K as yet, and it seems plausible that the reaction probability, as defined here, will increase again, e.g., because new, further away sites become accessible to the H atom, in particular when diffusion becomes appreciable. In addition to the maximum in the reaction probability in T, it is interesting also to note that the actual magnitudes of the cage-exit probability remain quite low over the temperature range studied. This is not in accord with available experimental data on HI photolysis in matrices at low temperature.[33] The most obvious explanation may be that matrices are far less "tight" than crystalline rare gas, and much of the observed cage exit of H atoms is due to defects, porous structure of the matrix, etc. It is, however, also conceivable that tunneling plays a major role in the exit of H atoms from the cage.[23] A conclusion on this very important question must await future experimental and theoretical studies.

TABLE I. Cage-exit probability of H vs temperature. The relative initial energy of the photofragments in the calculation was 1.5 eV, corresponding to photodissociation by a 4.55 eV photon.

Temperature (K)	Cage-exit probability
0°	0
17°	0.2
35°	0.1

D. Transient frequencies of photofragments

As Figs. 4–6 show, *the H atom executes large amplitude vibrations in the original cage for several picoseconds following photodissociation, even for trajectories that ultimately exit from that cage.* Such motions should be observable in principle, in both time-domain and frequency-domain experiments. Figure 7 shows Fourier transform, taken over the time interval from 0 to 0.45 ps after photodissociation, of the H atom trajectory described in Fig. 5. This corresponds to the early stage of the process, within which the H atom loses most of its kinetic energy (which decreases from 1.1 to 0.37 eV). The H motion in that time regime shows a pronounced pair of frequency peaks at ~ 400 and ~ 600 cm^{-1}, and a second well-defined pair of peaks at ~ 800 and ~ 900 cm^{-1}. All these high frequency peaks pertain to the oscillatory motion of the very energetic H fragment between the Xe walls of the cage. Typically, the frequency of a particle moving between repulsive walls increases with increasing energy. Therefore, the higher frequency peaks at ~ 800 and 900 cm^{-1}, are probably due to the earliest part of the time interval considered, when the H atom had energy of the order of 1 eV. Figure 8 shows the Fourier transform of the H fragment trajectory of Fig. 5, but for times $t>3.5$ ps (and up to 7 ps, for which the trajectory was calculated). As Fig. 5 shows, in this interval the H is already in the new cage, and has lost all but a small fraction of its kinetic energy of the initial stage. The nearly relaxed, low energy motions of the H atoms in the final cage account for the fact that the higher frequency peaks of Fig. 7 are not found in Fig. 8. The better resolution of the peaks in Fig. 8 is due to the much increased time interval over which the Fourier transform is taken. We conclude that the transient frequency spectrum of the H photofragment contains a wealth of information on the dynamics, and it should be highly desirable to try and measure it experimentally.

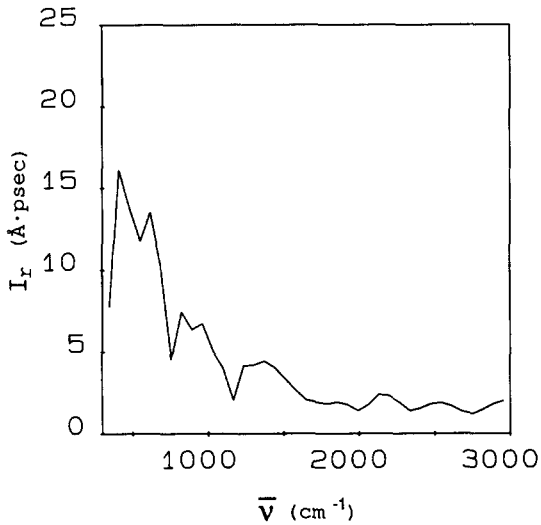

FIG. 7. Fourier transform $I_r(\bar{\nu})$ of the H atom trajectory $|\mathbf{r}(t)-\mathbf{r}_0|$ for $0<t\leqslant 0.45$ ps. The transformed trajectory is from Fig. 5.

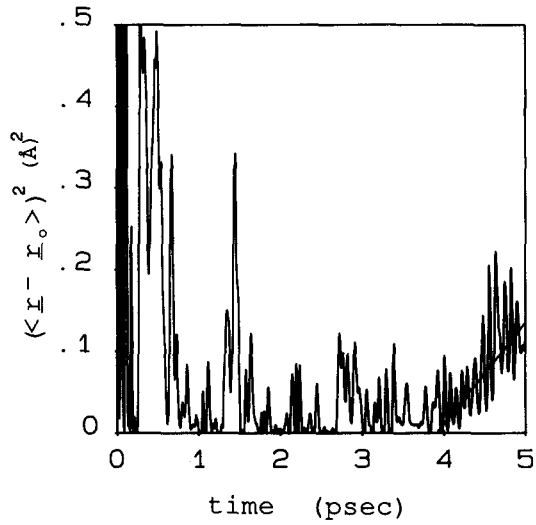

FIG. 9. Long-time diffusive behavior of H fragment trajectories. The results show $\langle|\mathbf{r}(t)-\mathbf{r}_0|^2\rangle$ vs t,$\mathbf{r}(t)-\mathbf{r}_0$ is the H distance from its initial position upon photon absorption. $\langle\cdots\rangle$ denotes average over all the calculated trajectories. The results are for $T=35$ K, the initial relative energy of the fragments was 1.5 eV. The fit to diffusive behavior is shown for $t>3.8$ ps.

E. A diffusive behavior of nonreactive trajectories

Figure 9 shows the time variation of $\langle[\mathbf{r}(t)-\mathbf{r}_0]^2\rangle$, where $\mathbf{r}$ is the H position at time t, $\mathbf{r}_0$ the initial H position upon photodissociation, and $\langle\cdots\rangle$ indicates an average over all the trajectories computed at that energy and temperature. The results shown are for $T=35$ K at which the reaction probability is low. The results thus mainly reflect the behavior of the trajectories that remain in the original cage. The most interesting aspect of Fig. 9 is the linear behavior observed, for long times, for $\langle(\mathbf{r}-\mathbf{r}_0)\rangle^2$ in t. A possible interpretation may be the following one. After the H atom has lost most of its kinetic energy, local heating of the environment must have taken place. We suggest that the "diffusive" behavior in Fig. 9 is due to a structural relaxation of the cage, that has been induced by the local heating. Note that the structural relaxation (to which the H atom responds, as seen in Fig. 9) is expected to be a slow process. The "diffusion coefficient" of 1.6×10^{-5} cm^2/s, extracted from the slope in Fig. 9, is typical of diffusion in liquids or in solids at very high temperature. This number seems consistent with the above interpretation.

F. Geometry and vibrations of H products at final site

We assume now that sufficiently long a time has passed, after the photodissociation event, and that relaxation to equilibrium has taken place. The question is what are the expected properties of the H product sites. For this purpose, we carried out simulations of H atoms in a host Xe crystal. We considered both octahedral (O_h) and tetrahedral (T_d) sites for the H atom within the fcc unit cell, as shown in Fig. 10. The simulations show that the dilation (or structural relaxation) introduced by the presence of the interstitial H are very large for both types of sites: The Xe atoms surrounding the H in the O_h site displace radially as shown in Fig. 11.

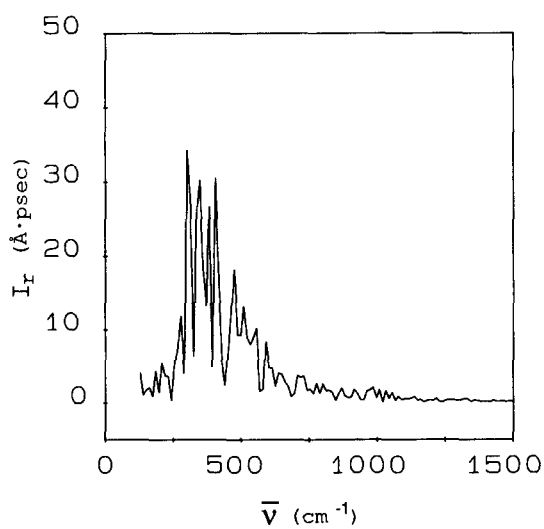

FIG. 8. Fourier transform $I_r(\bar{\nu})$ of the H atom trajectory for $3.5>t\geqslant 7$ ps. The results are for the same trajectory as in Fig. 5.

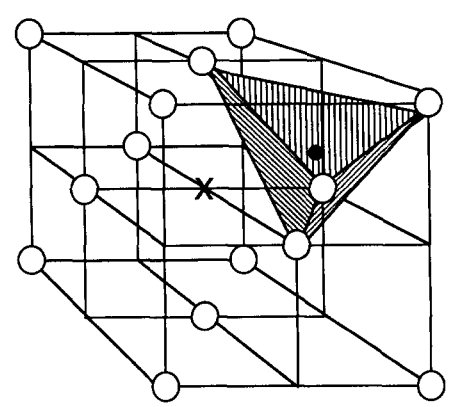

FIG. 10. Tetrahedral (shaded circle) and octahedral ($\times$) interstitial sites in fcc lattice.

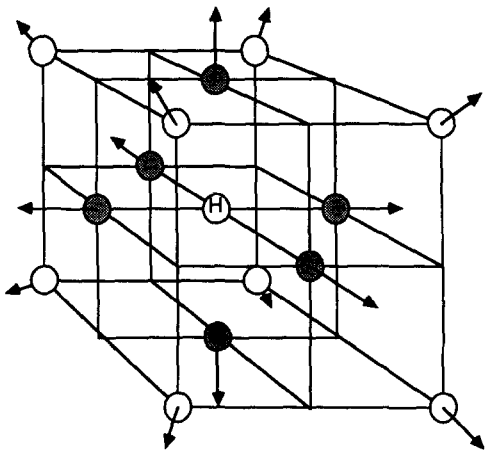

FIG. 11. The direction of distortions of lattice (structural relaxation) due to H atom impurity in O_h interstitial site of fcc lattice. The directions of the distortion are from the molecular dynamics calculation. The mean displacement of nearest-neighbor xenons (shaded circles) is 0.3 Å, while that of second nearest neighbors (open circles) is 0.15 Å.

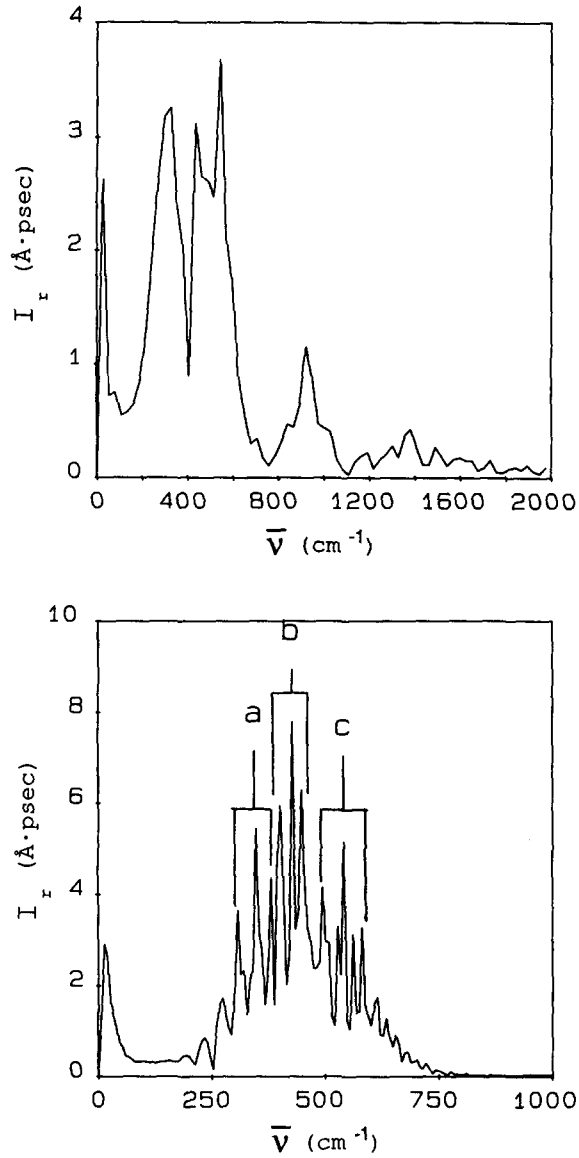

FIG. 12. (a) Fourier transform $I_r(\bar{\nu})$ of H atom trajectory $\mathbf{r}(t)$, at an O_h distorted site in a 17 K Xe lattice. The Fourier transform is a low resolution one, based on $\mathbf{r}(t)$ for $t<1.25$ ps only. (b) High resolution Fourier transform of H atom trajectory at a distorted O_h site. Calculation is for the same conditions as in (a), but using times $t<5$ ps. The main three peaks around 350, 450, and 550 cm^{-1} are now split due to combinations with lattice frequencies.

The tetrahedral interstitial site involves even larger distortions (nearest-neighbor Xe displacements of up to 0.6 Å). These large distortions greatly affect the calculated vibrational frequencies. Approximate calculations of the vibrations of an interstitial H that neglect relaxation, e.g., Ref. 34) are not valid in this case. Figure 12(a) shows the Fourier transform of an H atom trajectory for such a distorted O_h site (calculated lattice temperature of 1 K). The trajectory was calculated over 1.25 ps only, to provide first a Fourier transform at low resolution. We note the pronounced, but broad peaks at $\sim$350, $\sim$450, and $\sim$550 cm^{-1} which correspond to H vibrations. With this in mind, we proceed to Fig. 12(b) that shows a higher resolution transform calculated from a 5 ps trajectory. We recognize now a group of three peaks, the center of each corresponds to the frequencies of Fig. 12(a). Each of the other frequencies can be written as $\bar{\nu}_i = \bar{\nu}_{\mathrm{H}}^{(i)} \pm \bar{\nu}_{\mathrm{Latt}}$ where $\bar{\nu}$ is a lattice frequency (i labels each of the three main frequencies seen). In addition to the local H vibrations, Fig. 12(b) shows combinations of such vibrations with lattice modes. An important point to notice is the very large splitting, $\sim$100 cm^{-1} between the three frequencies of the H local vibrations. This is in considerable difference with the often used spherical cage approximation. Figure 13 provides an obvious explanation for the three different frequencies: they involve vibrations along the three main axes of the O_h cage. The vibration between the two (repulsive) Xe atoms is the stiffest. The second vibrational axis is between two pairs of Xe atoms, and the lowest frequency vibration is due to motion along the axis joining the faces of the octahedron. Vibrational motion in an undistorted, rigid octahedral site is expected to be degenerate. In the present case, there is a large dynamical distortion which lifts the degeneracy: The Xe atoms move, and their motions are coupled to that of the H, especially in view of the crowded site and the associated large repulsive interactions. The "nonadiabatic" effects that split the degeneracy are therefore especially large here. Measurement of such large splittings experimentally, should in principle be possible, and would provide information on sites and interactions of H atoms in a host crystal. We stress that this result could depend significantly on the interaction potential used, and on the distorted site geometry: A less "tight" site may not suffice to produce significant nonadiabatic splittings.

IV. CONCLUDING REMARKS

This article described molecular dynamics simulations of HI photodissociation in a host Xe crystal at finite temperatures. It is the first study of such a process in a crystalline medium. The study dealt with the behavior of the HI

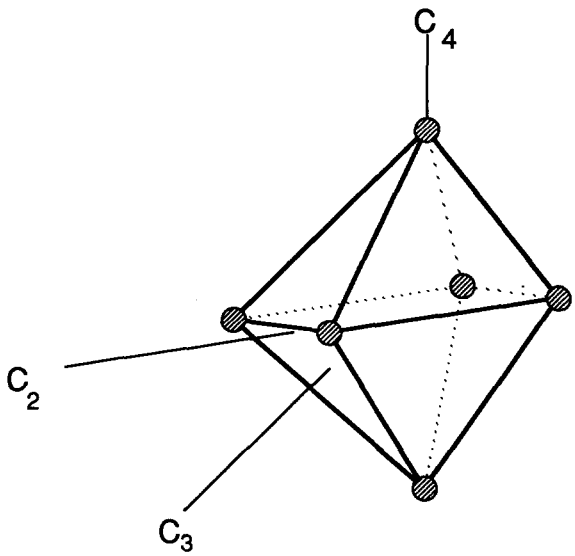

FIG. 13. The three axes for H vibrations in an O_h interstitial site. The corresponding frequencies are in the order $\bar{\nu}(C_4) > \bar{\nu}(C_2) > \bar{\nu}(C_3)$.

molecule before dissociation, the dynamics of the photofragments throughout the process, and the properties of the H product at its final, relaxed site.

Mechanistically, the main result we wish to emphasize is the fact that fragment exit from the cage is never a direct process in this system: This is always preceded by a long duration in which the H atom rattles in the original cage carrying out large amplitude motions and loosing the greater part of its initial kinetic energy. Only after several picoseconds of such vibrations may the H reach a sufficiently low barrier that it can surmount and exit the cage. This mechanism offers a useful guide for the development of statistical, transition state-type models for such processes. Closely related to this feature, and of considerable implications for future experimental studies, is that the H motion in the original cage at the early time interval following photodissociation ($t < 1$ ps) exhibits fairly well defined, and very high frequencies. Exploration of the transient frequency pattern over a short time scale in such systems appears to us a very promising experimental direction for exploring photodissociation dynamics. Another finding of potential experimental consequences is the nonmonotonic dependence of the cage-exit probability on temperature. Also, the relatively low magnitude of the exit probabilities (at temperatures $T \leqslant 35$ K) is of interest. This seems in marked contrast to the experimental situation for matrices, where cage exit appears a high probability event even at low temperature.[33] The difference may be due to defects in the matrix, to a less tight structure of the latter, or perhaps due to quantum tunneling effects that were ignored in the present calculations.[23] Clearly, there are many important questions on this process that await future experimental and theoretical work.

An essential question with regard to the classical dynamics method used here is that of the role of quantum effects. Obviously, tunneling, if significant, may enhance cage-exit probabilities, as mentioned above. Note, for instance, that in our calculations we found no true large scale diffusive motion of H atoms (beyond the nearest-neighbor cage): There is no thermal diffusion on our time scale. Quantum effects may perhaps give rise to tunneling diffusion. This is an extremely interesting point that merits attention. However, we note that, the presented results, at least with respect to dissociation probabilities at finite temperatures, are not expected to change by any significant extent. Estimates of tunneling in this system by one-dimensional action integrals,[35] indicate that tunneling proceeds on a time scale of 10^{-10} s, a time scale much longer than the observed cage-exit dynamics. Recombination is another potentially important nonclassical process (since it involves a transition between two electronic states of the HI system), although it can be treated by quasiclassical approximations. Finally, at the lowest temperatures, effects of the quantum zero-point vibrations of the atoms involved may become important. It is essential to try and deal with such effects in future studies. We are currently pursuing work where the H atom is treated by quantum-mechanical time-dependent wave packets, while the heavier atoms are still described by classical molecular dynamics. Such mixed quantum-classical treatments have recently been used quite extensively in molecule/surface scattering theory.[36] We hope that with the advent of such treatments, steps forward can be made in the incorporation of quantum effects.

ACKNOWLEDGMENTS

We should like to thank A. Brokman, J. Khademi, W. Lawrence, and M. E. Fajardo for many helpful discussions. R. B. Gerber gratefully acknowledges support from the Institute for Surface and Interface Science, of the University of California at Irvine, where most of this work was done. This work was supported by a contract from the U.S. Air Force Astronautics laboratory under Contract No. F04611-87-K-0024. The Fritz Haber Research Center of the Hebrew University of Jerusalem is supported by the Minerva Gesellschaft für die ferschung, München, Germany.

[1] J. T. Hynes, Annu. Rev. Phys. Chem. **36**, 573 (1985).
[2] K. V. Mikkelsen and M. A. Ratner, Chem. Rev. **87**, 113 (1987).
[3] H. Frei and G. C. Pimentel, Annu. Rev. Phys. Chem. **36**, 491 (1985).
[4] J. D. Baldeschwieler and G. C. Pimentel, J. Chem. Phys. **33**, 1008 (1960).
[5] P. Felder and Hs. H. Gunthard, Chem. Phys. **85**, 1 (1985).
[6] P. A. McDonald and J. S. Shirk, J. Chem. Phys. **77**, 2355 (1982).
[7] A. E. Shirk and J. S. Shirk, Chem. Phys. Lett. **97**, 549 (1983).
[8] M. Rasanen and V. E. Bondybey, J. Chem. Phys. **82**, 4718 (1985).
[9] M. Poliakoff and J. J. Turner, in *Chemical and Biological Application of Lasers*, edited by C. B. Moore (New York, Academic, 1980), Vol. 5, p. 175.
[10] H. Frei, L. Fredin, and G. C. Pimentel, J. Chem. Phys. **74**, 397 (1981).
[11] H. Frei and G. C. Pimentel, J. Chem. Phys. **78**, 3698 (1983).
[12] V. E. Bondybey and L. E. Brus, J. Chem. Phys. **62**, 620 (1975).
[13] L. E. Brus and V. E. Bondybey, J. Chem. Phys. **65**, 71 (1976).
[14] V. E. Bondybey and C. Fletcher, J. Chem. Phys. **64**, 3615 (1926).
[15] M. E. Fajardo and V. A. Apkarian, J. Chem. Phys. **85**, 5660 (1986).
[16] M. E. Fajardo and V. A. Apkarian, Chem. Phys. Lett. **134**, 51 (1987).
[17] L. Wiedmeman, M. E. Fajardo, and V. A. Apkarian, J. Phys. Chem. **92**, 342 (1988).
[18] R. B. Gerber and M. Berkowitz, Phys. Rev. Lett. **39**, 1000 (1977).
[19] M. Berkowitz and R. B. Gerber, Chem. Phys. **37**, 369 (1979).

[20]K. F. Freed, D. L. Yeager, and H. Metiu, Chem. Phys. Lett. **49**, 19 (1977).
[21]D. J. Diestler, E. W. Knapp, and H. D. Ladouceur, J. Chem. Phys. **68**, 4056 (1978).
[22]For a review see H. Dubost, in *Inert Gases*, edited by M. L. Klein, Springer Series in Chemical Physics 34 (Springer, Berlin, 1984), p. 145.
[23] R. Alimi, A. Brokman, and R. B. Gerber, in *Stochasticity and Intramolecular Distribution of Energy*, edited by R. Lefebvre and S. Mukamel (Reidel, Dordrecht, 1987).
[24]G. N. A. Van Veen, K. A. Mohammed, T. Baller, and A. E. De Vries, Chem. Phys. **80**, 113 (1983).
[25]R. D. Clear, S. J. Riley, and K. R. Wilson, J. Chem. Phys. **63**, 1340 (1975).
[26]R. S. Mulliken, Phys. Rev. **51**, 310 (1937).
[27]U. Buck, Adv. Chem. Phys. **30**, 314 (1976).
[28]R. W. Bickes, B. Lantszch, J. P. Toennies, and K. Walascheuski, Discuss. Faraday Soc. **55**, 167 (1973).
[29]G. Herzberg, *Spectra of Diatomic Molecules* (Litton, London, 1950).
[30]M. L. Klein, Annu. Rev. Phys. Chem. **36**, 525 (1985).
[31]H. Friedmann and S. Kimel, J. Chem. Phys. **43**, 3925 (1965).
[32]S. Nosé and M. L. Klein, Mol. Phys. **46**, 1063 (1982).
[33]K. Kinugawa, T. Miyazaki, and H. Hose, J. Phys. Chem. **83**, 1697 (1978).
[34]S. S Cohen and M. L. Klein, J. Phys. Chem. **67**, 2397 (1977).
[35]R. Alimi, thesis, The Hebrew Univeristy of Israel, Jerusalem, 1986, p. 61.
[36]R. B. Gerber, R. Kosloff, and M. Berman, Comput. Phys. Rep. **5**, 59 (1986).